AIP Conference Proceedings

RESEARCH ARTICLE | JANUARY 15 2019

High-flux XAFS-beamline P64 at PETRA III

Wolfgang A. Caliebe ✉; Vadim Murzin; Aleksandr Kalinko; Marcel Görlitz

Check for updates

AIP Conf. Proc. 2054, 060031 (2019)
https://doi.org/10.1063/1.5084662

View Online Export Citation CrossMark

Articles You May Be Interested In

The quick EXAFS setup at beamline P64 at PETRA III for up to 200 spectra per second

AIP Conference Proceedings (January 2019)

The PETRA III extension

AIP Conference Proceedings (July 2016)

A beamline for bulk sample x-ray absorption spectroscopy at the high brilliance storage ring PETRA III

AIP Conference Proceedings (January 2019)

21 September 2023 14:58:05

500 kHz or 8.5 GHz?
And all the ranges in between.
Lock-in Amplifiers for your periodic signal measurements

Find out more
Zurich Instruments

AIP Publishing

High-Flux XAFS-Beamline P64 at PETRA III

Wolfgang A. Caliebe[1,a)], Vadim Murzin[1], Aleksandr Kalinko[1,2] and Marcel Görlitz[1]

[1]*DESY, Notkestrasse 85, 22603 Hamburg, Germany*
[2]*Paderborn University, Warburger Str. 100, 33098 Paderborn, Germany*

[a)]Corresponding author: wolfgang.caliebe@desy.de

Abstract. Beamline P64 at PETRA III is dedicated to x-ray absorption spectroscopy experiments which require high flux, like quick extended x-ray absorption fine structure spectroscopy on the sub-second time scale, high-resolution resonant emission spectroscopy, and x-ray absorption fine-structure spectroscopy of highly diluted systems. The beamline is installed at the high-energy storage ring PETRA III. The source is a 2 m-long undulator. The beamline covers an energy-range from 4 keV to 44 keV, which was required by the user community. Mirrors can be used to reduce the intensity of higher harmonics, and to focus the beam. A conventional photo-diode and a 100-pixel high-purity Ge-detector are used in fluorescence extended x-ray absorption fine-structure spectroscopy for diluted samples.

21 September 2023 14:58:05

INTRODUCTION

X-ray Absorption Spectroscopy (XAS) is a unique method for element-specific studies of materials. Although the basic idea of measuring the absorption coefficient with X-rays and the first spectrum of an absorption edge are more than 100 years old [1], the method is constantly evolving. The applications of XAS at first were limited by its photon hungriness. The appearance of synchrotron radiation sources has brought XAS to a more advanced level, drastically decreasing time for acquisition of X-ray Absorption Near Edge Structure (XANES) and Extended X-ray Absorption Fine Structure (EXAFS). It has opened the possibility of more sophisticated methods to develop. New instrumentation at synchrotron radiation beamlines is also improving. As a variation of XAS today we have: Quick EXAFS (QEXAFS), High Energy Resolution Fluorescence Detected XAS (HERFD-XAS), Resonant X-Ray Emission Spectroscopy (RXES), and Valence-To-Core X-Ray Emission Spectroscopy (VTC-XES). Nevertheless, it is always a trade-off between the concentration of the element in the sample, the time resolution, and the energy resolution of the spectra. For the best performance one benefits to have the maximum number of incident photons which the sample can handle without being modified.

In this paper, we present the new Beamline P64 located at PETRA III, DESY's synchrotron radiation facility (Hamburg, Germany) [2, 3]. It is dedicated to XAS experiments which require high flux like EXAFS of highly diluted systems, QEXAFS measurements on a timescale of 10 ms – 10 s, and RXES, which help to overcome the lifetime broadening of the core-hole. We describe the instrumentation installed at the beamline, discuss various scanning techniques, and present some experimental results.

X-ray Source and X-ray Optics

In order to deliver high flux to the sample, a tunable X-ray source with high spectral brightness, cryogenically cooled monochromators, and additional optical components are required in order to tailor the beam to the desired properties. A schematic layout is given in figure 1. Detailed information on the various components in the front-end of the beamline are given in [4]. The distances of the main components to the middle of the undulator are given in table 1.

Proceedings of the 13th International Conference on Synchrotron Radiation Instrumentation – SRI2018
AIP Conf. Proc. 2054, 060031-1–060031-6; https://doi.org/10.1063/1.5084662
Published by AIP Publishing. 978-0-7354-1782-3/$30.00

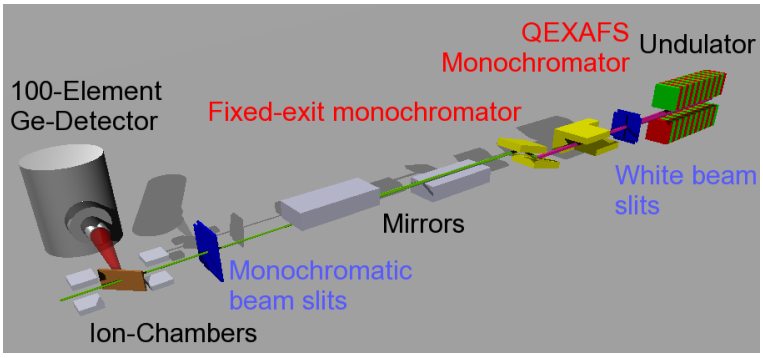

FIGURE 1. Schematics of beamline: A 58-pole undulator emits synchrotron radiation. A pair of slits selects the central cone, and two different monochromators can select the required wave-length for the experiment. Two mirrors reject higher harmonic radiation, and can focus the beam, if it is required. An additional pair of slits selects the part of the beam, which is used for the experiment. The intensities of the incident and transmitted beams are measured by two ion-chambers, respectively, and the fluorescence signal can be measured by a 100-pixel high-purity Ge-detector.

TABLE 1. Distances of optical components from the source (middle of undulator).

Component	Slit I (v)	Slit II (vxh)	Filter	Shutter	Q-Mono	DCM	Mirror I	Mirror II	Slit III (vxh)	Sample
Distance/m	37.1	44.8	45.6	48.9	52.4	56.6	58.7	60.5	87	87.2

Undulator

The radiation-source is 2 m-long, 58-pole undulator with a period of 32.8 mm [5]. The period was chosen such that it is possible to measure the K-absorption edge of all 3d-metals without a change of the harmonic and with a reduction of flux by less than a factor of 5. Calculations using Spectra 9.0 [6, 7, 8] show that this is indeed the case, and that there is a rather large overlap of the first and third harmonic. The calculated spectral flux for the first 11 harmonics is shown in figure 2a.

Additionally, the spectrum of the tapered undulator covers an energy range of more than 1 keV for all 3d-elements heavier than Mn. We have also used even harmonics in the tapered configuration for some measurements, where an odd harmonic did not deliver the required energy-range. The velocity of the motors, which adjust the gap, can be controlled while the motors are moving. This feature is essential for continuous energy scans, where the monochromator and undulator are moved simultaneously.

Monochromators

Beamline P64 is special since it has two independent cryogenically-cooled monochromators, which are optimized for different applications. The first monochromator is a channel-cut monochromator (CCM), which can oscillate with frequencies up to 20 Hz (50 Hz) for Quick-EXAFS (Quick-XANES). This monochromator is described in detail in [9] and [10]. In brief, the gap has a width of 12 mm for a beam-offset of at least 21 mm at high energies. This results in a vertical beam-translation of 140 μm for an EXAFS-scan at the Fe K-edge which starts 200 eV below the edge and extends up to 1000 eV above the edge.

The second monochromator is a double-crystal fixed-exit monochromator (DCM), which has been designed by Oxford Ltd.. The design is based on the previous design for the first x-ray beamlines at PETRA III [11], with a few modifications to reduce the oscillations of the second crystal [12]. In short, both monochromator crystals are cooled to liquid nitrogen temperature in order to reduce lattice strain by the heat-load impinging on the first crystal. The relative position of the two crystals is adjusted in order to keep the vertical beam-position fixed. The tilt (pitch) of the second crystal can be controlled with a piezo-actuated tilt-stage, which can be used for a feed-back system to stabilize the intensity or beam-position.

Two different crystal-pairs are installed in both monochromators (CCM and DCM) for different energy ranges: The crystal pairs in the DCM cover an energy range of 2.4 – 54 keV (Si(111)), and 4.6 – 103 keV (Si(311)). In order to reach low energies (large Bragg-angles) with the DCM, the first monochromator crystal has to be moved physically

21 September 2023 14:58:05

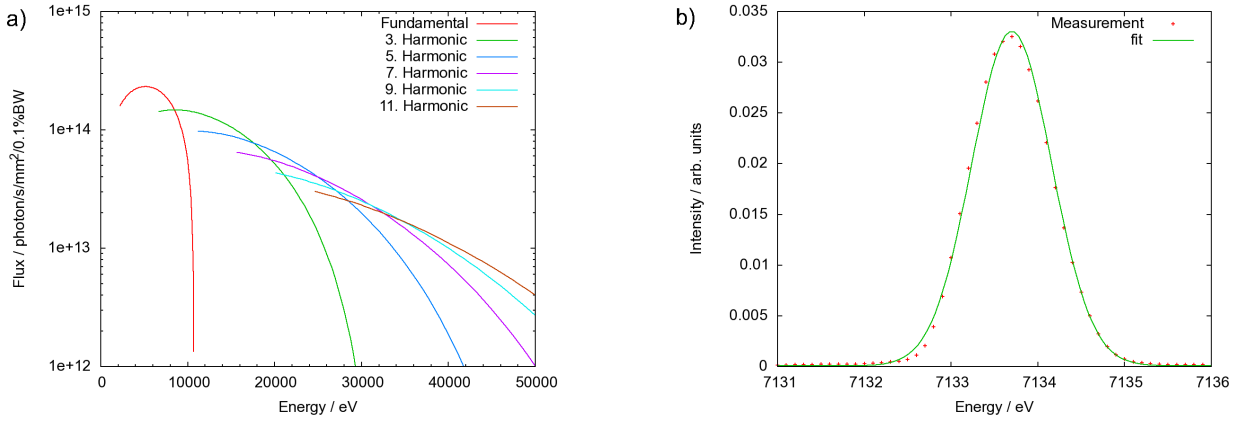

FIGURE 2. a) Flux of the 2m-undulator on the sample as a function of energy. Just the central cone with a size of about 1 mm^2 at the position of the sample is used.
b) Energy-resolution of the Si(111) fixed-exit monochromator at an energy of 7133.8 The quasi-elastic scattering was measured with the von-Hamos spectrometer. The measured and calculated energy resolutions agree perfectly.

towards the beam. Otherwise, the downstream part of the first monochromator crystal blocks the monochromatic beam, which is reflected by the second crystal. So far, the monochromators have been tested in the energy range from 4 – 40 keV. The flux on the sample is as high as 10^{13} photon·s^{-1} in the energy range of the 3d-metals with the Si(111) monochromator, and a factor of 5 lower for the Si(311) monochromator.

The CCM covers an energy range of 4 – 22.7 keV (Si(111)), and 7.6 – 43 keV (Si(311)). The flux on the sample of the CCM compared to the DCM is a factor of 2.5 lower for the Si(111) monochromator, and a factor of 10 lower for the Si(311) monochromator. Since we have to taper the undulator in order to broaden the energy spectrum, we lose an additional factor of 10 in flux for QEXAFS-experiments.

The energy resolution of the Si(111)-reflection is $\Delta E/E=1.4\cdot10^{-4}$, which corresponds to 1 eV at 7.1 keV. Since a high-resolution dispersive von-Hamos spectrometer is installed at the beamline, we could confirm this value for the DCM with a direct measurement of quasi-elastic scattering, which is shown in figure 2b. The fit has a width of 1.1 eV, which corresponds to the convolution of the energy width of the incident beam (1 eV) with the energy-resolution of the spectrometer (0.5 eV) in that configuration. We also measured in a similar way the energy resolution of the Si(311)-monochromator at 8 keV with the Si(444)-crystal as analyzer, and we determined a value of 240 meV for the monochromator, which corresponds to the intrinsic value of $\Delta E/E=3\cdot10^{-5}$.

Mirrors

Two Si-mirrors with a length of 800 mm are installed downstream of the monochromators. Their main purpose is to reduce the intensity of higher harmonics. Therefore, three different coatings over a length of 500 mm are used for different energy ranges: No coating (bare Si) for the lower, Rh for the intermediate, and Pt for the higher energy range. This way, it is possible to avoid artifacts in the EXAFS-spectra which can be induced by absorption edges of the mirror-coating. The suppression of higher harmonics for the Si-stripe is as high as $2\cdot10^{-5}$ at 5 keV, and still $2\cdot10^{-3}$ at 8 keV for the Rh-stripe, if one includes the significantly lower reflectivity of the Si(333) reflection compared to the Si(111) reflection. If the flat stripes are used, one can increase the angle of incidence and thus improve the suppression.

Additionally, the mirrors can be used to focus the beam. For that purpose, two grooves with different radii are machined in the first mirror for horizontal focusing. The first one is un-coated (bare Si) for the low energy range, and the second one is coated with Rh for the intermediate energy range. Therefore, it is possible to focus the beam horizontally in the energy range of 2.4 keV to 22 keV. The second mirror can be bent for vertical focusing over the entire energy range. Parameters for the mirrors are given in table 2.

So far, we were not able to focus the beam to the calculated values. We measured a horizontal width of 150 μm, and especially the measured vertical beamsize is significantly larger with 50 μm than the calculated one. We attribute this to some residual beam-vibrations, and to small imperfections in the mirrors. The influence by vibrations might be reduced by a feedback-system on the position of the beam. Due to the rather large beam-motion of the CCM,

21 September 2023 14:58:05

we have not used it so far in combination with the mirrors. Typical beamsizes in experiments with the CCM were 1.5 mm x 0.7 mm.

TABLE 2. Mirror parameters and beamsize (ray-tracing results) for two different positions in the experimental hutch. It is also always possible to use the flat sections of the mirrors, which give a beamsize of approximately 1.5x0.75 mm^2.

E-range / keV	EXAFS	RXES	Angle / mrad	Reflec.	Coating	Radii (km, mm)	Beamsize (hxv) / μm^2
4 – 9	X		3.3	>85%	Si	9.6, 109	92 x 14
		X	2.8		Si	13.2,109	120x21
7 – 20	X		3.0	>85%	Rh	10.6, 99	93x14
		X	2.6		Rh	14.6, 99	120x21
15 – 40	X	X	2.0	>70%	Pt	∞	1500x700
35-45	No mirror						1500x300

Detectors

The standard detectors in an EXAFS-beamline are ion-chambers which measure the incident and transmitted flux on the sample [13]. For lower concentrations or thick samples, a passivated implanted planar silicon (PIPS) detector [14] can be used. For highly diluted samples, a 100-element highly-purified planar Ge-detector is used. By using appropriate combination of filters, which can reduce fluorescence by lower-Z elements or which reduce elastic and Compton scattering, the application range of the PIPS-detector can be increased significantly and the signal-to-background quality of the Ge-detector can be improved as well.

The high-purity 100-pixel monolithic Ge-detector was manufactured by Canberra [14]. We use Struck-3302ADC cards [15] to read the signal directly from the pre-amplifier. These cards deliver an entire energy spectrum, and provide the possibility to analyze intensities in specified regions of interest. Reading and saving the energy spectrum takes less than 300 ms for all 100 pixels. Different methods have been tested to extract better data from the entire spectrum than the usual region of interest. In a few cases, it is advantageous to fit the line-shape of the elastic scattering line as a background in order to extract the pure fluorescence signal [16, 17].

In recent years, high-resolution emission spectroscopy and resonant x-ray emission spectroscopy developed into complementary tools to XAFS due to the high flux at modern XAFS-beamlines and developments in detector and in crystal analyzer technology. Therefore, a dispersive von-Hamos spectrometer was installed at the beamline. The horizontal scattering geometry was chosen since it facilitates the installation of different sample environments, and allows mounting detectors in a more stable way. The scattering angle is fixed at 90°, which limits the applications to the study of emission lines. The spectrometer is described in detail in a separate presentation [18].

Sample environment

Since XAFS finds application in various field of research, different sample environments are required, which are quite specific for each experiment. The beamline provides different types of cryostats for cooling samples down to liquid nitrogen or helium temperatures, and it is possible to mount heating devices from the PETRA III sample environment pool. Recently, a liquid-jet and a closed liquid flow-cell for air-sensitive liquid samples were developed and successfully used for experiments. Several user groups come with their own reaction chambers for in-situ/in-operando experiments, and they profit from the infrastructure for gases, which allows them to study toxic and hazardous gases. In the nearer future, a laser will be installed in collaboration with several university-groups for pump-probe experiments. These experiments will profit from the high current in a single bunch in 40–bunch timing mode with a separation of 192 ns between two pulses.

Table 3 gives an overview of the different fields of research of the external user groups, and their main method during the experiment at Beamline P64 during the first three semesters of operation.

21 September 2023 14:58:05

TABLE 3. Overview of different research fields and required spectroscopic method at P64 from May 5, 2017 – July 17, 2018.

	Conv. EXAFS	QEXAFS	highly diluted	Spectrometer
Chemistry and Catalysis	2	6		8
Electro-Chemistry	7		1	
Biology, Life Sciences			4	
Environmental and Geo-Sciences	2			
Material Science and Physics	5	3	1	2

Experimental Results

In addition to conventional step-scans, we implemented continuous energy scans where the energy of the incident beam is tuned through the entire energy range, and the intensities of the detectors and the Bragg-angle of the monochromator are recorded on-the-fly. The rotation-speed of the monochromator is constant, and the undulator gap follows. Here, it is advantageous that the speed of the motors for the undulator-gap can be changed while the undulator is moving. Thus, it is possible to keep the nominal difference of the energy of the emitted (undulator) and diffracted (monochromator) photons to less than 2 eV, which is sufficient for all applications. The dead-time for accelerating, moving and stopping motors does not contribute to the measurement time of one EXAFS-spectrum. Figure 3 shows three EXAFS-spectra of a Cu-foil (left) and the XANES-spectrum (right), which were measured at a temperature of 20 K in transmission mode in 600 s up to 25 $Å^{-1}$ (2500 eV above the edge). All three spectra overlap even at highest momentum transfers and also in the XANES-region, which demonstrates the stability of the beamline. Usual scans up to 15 $Å^{-1}$ take 150-300 s. Step scans are only used in combination with the Ge-detector and the spectrometer, when longer counting times at each energy point are required. In that situation, the dead-time of motor motions is reasonably smaller than the counting time.

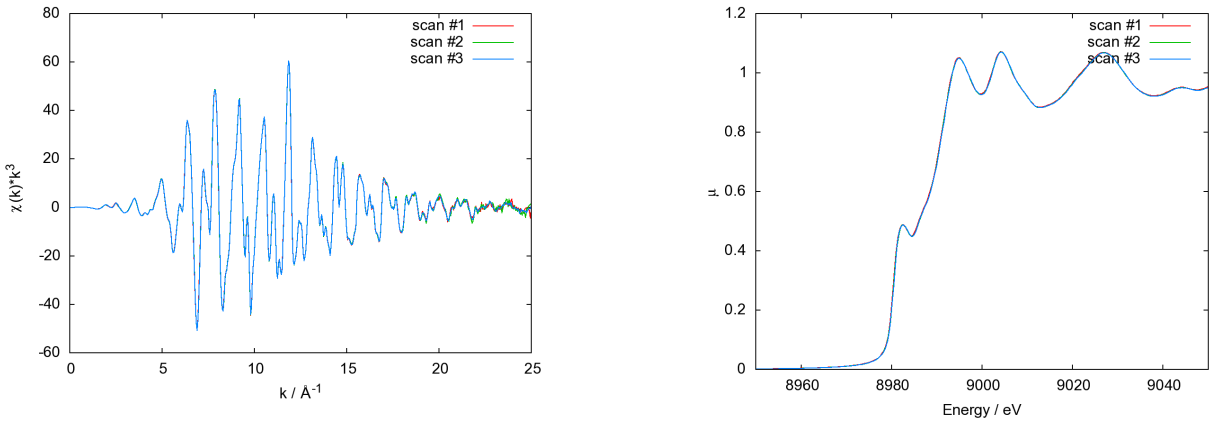

FIGURE 3. Cu EXAFS (left) and Cu-XANES (right) of a Cu-foil measured in transmission mode at a temperature of 20 K. Three consecutive scans are shown.

Conclusions

The high-flux EXAFS beamline P64 at PETRA III is a versatile instrument for applications of hard x-ray spectroscopy in chemistry, material and life sciences, physics, and related disciplines. This manuscript describes the beamline's optical configuration and performance. Most design-parameters have been reached. Some ways to improve the performance in the near future have been presented, as well as new installations.

21 September 2023 14:58:05

ACKNOWLEDGMENTS

DESY is supported by the German Ministry for Research and Education (BMBF) within the Helmholtz-Association. We would like to thank our colleagues from the beamline technology, experimental computing and undulator technology groups for excellent support. Discussions and collaborations on technical problems with our colleagues from the Applied XAFS Beamline P65 (Edmund Welter, Roman Chernikov, Ruidy Nemausat and Mathias Herrmann) and other beamlines at PETRA III are greatly acknowledged. Ligia Andrea Martin-Montoya tested different procedures to reduce the data from the 100-element Ge-detector and to optimize the signal-to-noise ratio. Suggestions by many scientists around the world helped in the design of the beamline. WAC would like to thank especially Jon Tischler for the suggestion to look also at even harmonics with a tapered undulator. We also want to thank our users for great publications!

REFERENCES

1. M. deBroglie, Comptes Rendus. **157**, 924–926 (1913).
2. H. Franz, O. Leopold, R. Röhlsberger, S.V. Roth, O.H. Seeck, J. Spengler, J. Strempfer, M. Tischer, J. Viefhaus, E. Weckert and T. Wroblewski, Synchrotron Radiat. News **19**, p. 2529 (2006).
3. W. Drube, M. Bieler, W. A. Caliebe, H. Schulte-Schrepping, J. Spengler, M. Tischer, and R. Wanzenberg, "The PETRA III extension," in *Proceedings of the 12th International Conference on Synchrotron Radiation Instrumentation – SRI2015*, AIP Conference Proceedings 1741, edited by Q. Shen and C. Nelson (American Institute of Physics, Melville, NY, 2016), pp. 020035–1–4.
4. H. Schulte-Schrepping, M. Hesse, M. Degenhardt, H. Krüger, R. Peters, H. B. Peters, and B. Steffen, "Photon beamline frontends for the PETRA III extension project," in *Proceedings of the 12th International Conference on Synchrotron Radiation Instrumentation – SRI2015*, AIP Conference Proceedings 1741, edited by Q. Shen and C. Nelson (American Institute of Physics, Melville, NY, 2016), pp. 020041–1–4.
5. A. Schöps, P. Vadin, and M. Tischer, "Properties of the insertion devices for PETRA III and its extension," in *Proceedings of the 12th International Conference on Synchrotron Radiation Instrumentation – SRI2015*, AIP Conference Proceedings 1741, edited by Q. Shen and C. Nelson (American Institute of Physics, Melville, NY, 2016), pp. 020019–1–4.
6. T. Tanaka and H. Kitamura, J. Synchrotron Rad. **8**, 1221–1228 (2001).
7. T. Tanaka, Phys. Rev. ST – Accel. Beams **17**, p. 060702 (2014).
8. T. Tanaka, Opt. Lett. **42**, 1576–1579 (2017).
9. O. L. Müller, "Hard X-ray Synchrotron Beamline Instrumentation for Millisecond Quick Extended X-ray Absorption Spectroscopy," Ph.D. thesis, Wuppertal University 2016.
10. B. Bornmann and R. Frahm, "The QEXAFS-Monochromator at P64 at DESY," in *13th International Conferenc on Synchrotron Radiation Instrumentation – SRI2018*, AIP Conference Proceedings, edited by S. Gwo, D.-J. Huang, and D.-H. Wei (American Institute of Physics, Melville, NY, 2019).
11. H. Schulte-Schrepping, M. Degenhardt, H.-B. Peters, U. Hahn, J. Heuer, and M. Hesse, "Status of PETRA III photon beamline frontends and optical systems," in *11th International Conference on Synchrotron Radiation Instrumentation (SRI 2012)*, Journal of Physics: Conference Proceedings 425, edited by P. Dumas and J. Susini (IOP Publishing Ltd., 2013), pp. 04205–1–5.
12. P. Kristiansen, J. Horbach, R. Döhrmann, and J. Heuer, J. Synchrotron Rad. **22**, 879–885 (2015).
13. G. Bunker, *Introduction to XAFS* (Cambridge University Press, Cambridge, 2010), pp. 63–71.
14. MIRION TECHNOLOGIES (CANBERRA) SAS, 1 Chemin de la Roseraie, 67380 Lingolsheim, France ().
15. Struck Innovative Systeme GmbH, Harksheider Str. 102A, 22399 Hamburg, Germany ().
16. L. A. Martin-Montoya, A. Rothkirch, and W. Caliebe, "Data reduction for XAS experiments with the 100 element Ge Detector," 16. International Conference on X-ray Absorption Fine Structure, Karlsruhe (Germany), 23 Aug 2015 - 28 Aug 2015 (IOP Publ., Bristol, 2016) p. 012016.
17. L. A. Martin-Montoya, "Automatic reduction of large x-ray fluorescence data-sets applied to XAS and mapping experiments," Ph.D. thesis, Paderborn University 2016.
18. A. Kalinko and M. Bauer, unpublished (2018).

21 September 2023 14:58:05